

## Bilinear and biquadratic exchange coupling in bcc Fe/Cu/Fe trilayers: Ferromagnetic-resonance and surface magneto-optical Kerr-effect studies

B. Heinrich, Z. Celinski, J. F. Cochran, A. S. Arrott, and K. Myrtle  
*Physics Department, Simon-Fraser University, Burnaby, British Columbia, Canada V5A 1S6*

S. T. Purcell\*

*Philips Research Laboratories, Eindhoven, The Netherlands*

(Received 28 July 1992; revised manuscript received 5 October 1992)

Ferromagnetic-resonance (FMR) and surface magneto-optical Kerr-effect (SMOKE) studies of the exchange coupling in bcc Fe/Cu/Fe(001) structures are presented. It is shown that the interfaces in bcc Fe/Cu/Fe(001) trilayers grown on a Ag(001) single-crystal substrate can be significantly improved by choosing an appropriate growth procedure. Low-energy electron-diffraction data are presented, which show that the bcc Cu(001) overlayer follows a nearly perfect bcc lattice. The exchange coupling in bcc Fe/Cu/Fe trilayers was studied as a function of interlayer thickness ranging from 7 to 14 monolayers. Quantitative data from FMR and SMOKE measurements are compared. The interpretation of magnetization loops for Fe/Cu/Fe trilayers requires the simultaneous presence of bilinear and biquadratic exchange coupling between the magnetic layers. Computer calculations were used to determine the strength of the bilinear and biquadratic exchange couplings. It is shown that the strength of the biquadratic exchange coupling increases with increasing terrace width. The measured values of the bilinear and biquadratic exchange coupling were compared with a model recently proposed by Slonczewski, which treats the exchange coupling in trilayers with imperfect interfaces. Slonczewski's model was used to deconvolute the data to obtain the intrinsic behavior of the bilinear exchange coupling in bcc Fe/Cu/Fe(001) trilayers. It is shown that the exchange coupling unobscured by interface roughness exhibits a strong short-wavelength oscillatory behavior that is in agreement with recent first-principles band calculations. Composite Ag-Cu structures were also studied. The presence of a few atomic layers of Ag(001) added to the Cu layer rapidly decreases the exchange coupling.

### INTRODUCTION

The study of the exchange interaction between ultrathin ferromagnetic layers separated by ultrathin nonferromagnetic interlayers has enjoyed a great deal of attention from both theorists and experimentalists. The exchange coupling through nonferromagnetic interlayers is strongly affected by the interface roughness. The ability to observe short-period oscillations i.e., oscillations on the scale of 2–3 monolayers (ML), depends sensitively on the quality of the interfaces.

The role of interface roughness has been recently treated by Slonczewski.<sup>1</sup> Slonczewski showed that when the exchange interaction changes rapidly with the number of monolayers and the interface consists of randomly distributed atomic terraces, then an additional term  $-J_1 \sin^2 \theta$  arises in the effective exchange interaction which couples two ferromagnetic layers through a nonmagnetic interlayer:

$$E = -J_0 \cos \theta - J_1 \sin^2 \theta, \quad (1)$$

where  $\theta$  is the angle between the magnetic moments and  $J_1$  is always positive: it is commonly known as the biquadratic exchange energy. Its presence in ultrathin films was first identified experimentally in the studies of the exchange interaction in the bcc Fe/Cr/Fe (Ref. 2) and in the fcc Co/Cu/Co(001) (Ref. 3) systems where the

equivalent effective exchange energy was written as

$$E = -(J_0 - J_1 \cos \theta) \cos \theta. \quad (2)$$

Our studies of the exchange coupling were carried out using ferromagnetic-resonance (FMR) and surface magneto-optical Kerr-effect (SMOKE) techniques. The intention of this paper is to present our studies of the exchange coupling in bcc Fe/Cu/Fe(001) trilayers in which the first Fe layer was grown at elevated substrate temperatures in order to decrease the number of atomic steps and thereby to increase the area of the individual atomic terraces at the Fe/Cu interface. The results on these samples will be compared with trilayers which were grown entirely at room temperature: in these trilayers the interfaces consist of many terraces of smaller area.

As the role of the interfaces is important to all aspects of this work, the paper starts with a discussion of growths studied using reflection high-energy electron diffraction (RHEED). Low-energy electron-diffraction (LEED) studies of the bcc Cu interlayer are also presented. Next, values of  $J_0$  and  $J_1$  are extracted from the magnetization loops measured using SMOKE. Quantitative results for the exchange coupling as obtained from the FMR and SMOKE studies will be compared for individual specimens.

The strength of the bilinear and biquadratic exchange interactions and their thickness dependences will be dis-

cussed within the framework of Slonczewski's model.<sup>1</sup> The samples with many small area terraces at the Fe/Cu and Cu/Fe interfaces result in an effective averaging out of the short-wavelength oscillations, while samples in which the interfaces are characterized by larger atomic terraces exhibit more pronounced short-wavelength oscillations in the exchange coupling. It will be shown that the Slonczewski model can be used to extract the intrinsic bilinear exchange coupling despite the interface roughness and therefore one can extract the change in the exchange interaction for a change of 1 ML in thickness. The results of these analyses show that the bilinear exchange coupling in bcc Fe/Cu/Fe(001) trilayers exhibits both short- and long-wavelength oscillations. The thickness dependence of the measured exchange coupling will be compared with recent first-principles calculations.<sup>4</sup>

Comparison with our previous studies<sup>5</sup> showed that the coupling in Fe/Ag/Fe ultrathin trilayers exhibited quite different behavior than Fe/Cu/Fe trilayers despite similarities between the Cu and the Ag valence bands. The Fe/Ag/Fe(001) trilayers grown at room temperature exhibited only ferromagnetic coupling which, with increasing interlayer thickness, reached a zero value by 7 ML. It will be shown that just two Ag(001) atomic layers added to the Cu(001) spacer layer between two iron films was enough to destroy the strong antiferromagnetic coupling through Cu.

### GROWTH STUDIES

The preparation of Ag(001) substrates has been described in previous papers.<sup>6</sup> Here we will summarize only those aspects and ideas which are relevant to the experiments discussed in this paper. The experiments were carried out in a PHI-400 MBE machine equipped for RHEED and Auger electron spectroscopy. The RHEED studies showed that the Fe growth on Ag(001) at room temperature (RT) proceeds in a quasilayer by layer growth in which the surface roughness is confined to the last two atomic layers.<sup>7</sup> The Fe growths on Fe(001), Cr(001), and Ag(001) templates at room temperature exhibit a well-defined splitting in the RHEED streaks, see Fig. 1(a). The shape of the observed streak splitting is characteristic of the intersection of Ewald's sphere with reciprocal rods consisting of alternating segments of hollow cylinders and straight lines. We refer to this structure as the Henzler structure, for it was observed by Hahn, Clabes, and Henzler<sup>8</sup> in their LEED studies of W(011) grown on W(011), and explained by them to be the result of the formation of clusters of atoms in one-atom-high islands with a strong correlation of the distances of separation of the island centers. The RHEED specular beam spot of the Fe(001) layers exhibits a significantly stronger intensity when it is located centrally between the split streaks. The corresponding RHEED intensity oscillations are in this case either very weak or even absent. This result suggests that the center of the split streaks corresponds to the Bragg reflection region. This is contrary to the conclusion of Hahn, Clabes, and Henzler<sup>8</sup> in which the diffraction cylinders are assumed to be centered in the anti-Bragg region. However, one

should point out that the RHEED diffraction intensities in stepped surfaces are very strongly affected by the presence of Kikuchi bands and consequently the interpretation of RHEED streak intensities is very complex.

The RHEED streak splittings represent a characteristic lateral spacing. It can be shown by a computer simulation that the reciprocal of the RHEED streak splitting is proportional to the average spacing between atomic islands (terraces). The inverse value of the observed RHEED splitting suggests that an average minimum separation between atomic islands is  $\sim 6$  nm for RT growth. When Fe(001) is grown on a Ag(001) substrate possessing atomic terraces which are smaller than  $60 \text{ \AA}$ , the Fe-atom positions are distorted by the vertical mismatch between Ag and Fe. The preparation of Ag(001) substrates is rather difficult. Ag single crystals are very soft and a Ag(001) substrate which has undergone mechanical polishing exhibits a badly damaged surface region. We

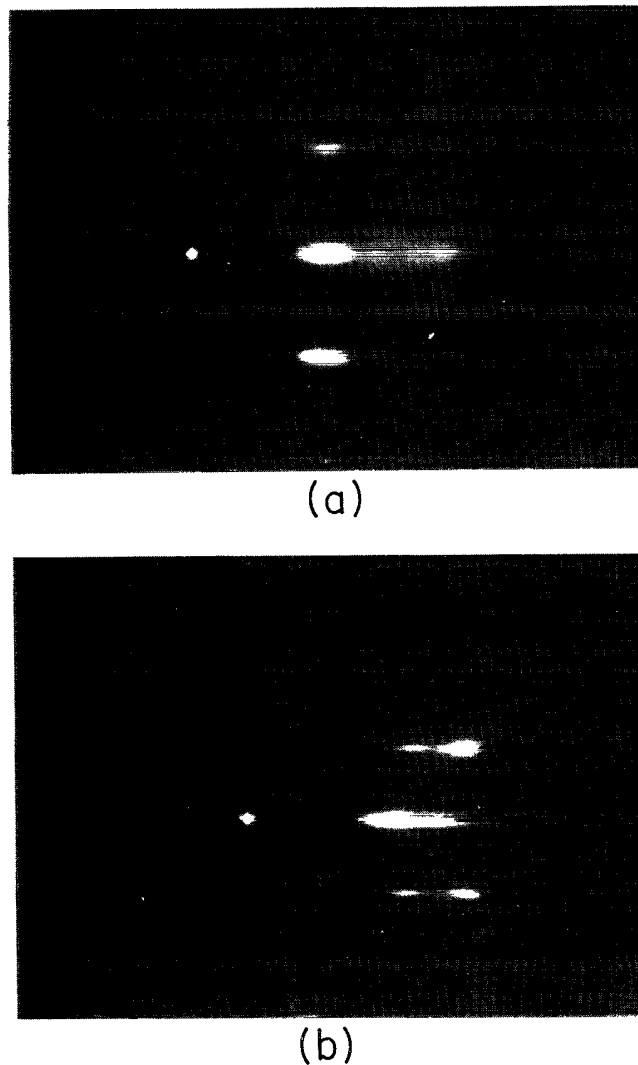


FIG. 1. RHEED patterns: (a) along a  $\{110\}$  azimuth for a 5.7 ML-thick bcc Fe(001) layer grown on a Ag(001) single-crystal substrate at room temperature; (b) along a  $\{100\}$  azimuth for 3.2 ML-thick Fe(001) grown on an Fe(001) template at 415 K.

found that it is necessary to remove a layer several  $\mu\text{m}$  thick by means of a proper electropolishing procedure<sup>9</sup> before the substrate is subjected to a UHV annealing and sputtering treatment. Substrates which have only been mechanically polished prior to a UHV treatment do not possess large atomic terraces. Scanning tunnel microscope (STM) studies of Ag(001) substrates prepared by mechanical polishing and subsequently treated by a UHV sputter-annealing procedure without electropolishing did not show well-defined atomic terraces at all, but yet they exhibited good LEED patterns.<sup>10</sup> Such samples show unacceptable RHEED patterns, and no sign of RHEED oscillations during growth.

The good lateral match between the Fe(001) and Ag(001) lattices in the plane is not found for the vertical direction. The difference in the vertical stacking between the fcc and bcc lattices results in a large vertical mismatch of approximately 16%. The growth of bcc Fe(001) on fcc Ag(001) templates with a high density of atomic steps is strongly affected by this large atomic vertical mismatch. In order to maintain good growth one has to use Ag(001) substrates characterized by atomic terraces which are significantly larger than the average Fe(001) nucleation site separation. Substrates with atomic terraces of several tens of nm are required to grow good ultrathin epitaxial Fe(001). In all our growths the first few atomic layers of Fe(001) are affected by Ag(001) substrate atomic steps. At least 3–4 ML of Fe have to be deposited in order to heal the distortions produced by the mismatch at the atomic steps. After 5–6 atomic layers of Fe(001), a constant periodicity in the RHEED intensity oscillations is achieved. Ag substrates which have shorter atomic terraces are more severely affected by Ag(001) substrate atomic steps and much thicker Fe(001) layers are required to reach an observable epitaxy.<sup>11</sup> The vertical mismatch problem mentioned above does not arise for bcc Fe grown on bcc Cu.

The growth of Fe(001) on Fe(001), Ag(001), and Cr(001) templates [all having a good lateral match to bcc Fe(001)] proceeds in the manner described above. At room temperature the nucleation centers of a newly forming atomic Fe(001) layer are separated approximately by 6 nm (determined from the RHEED streak splitting). When a Cu layer is grown on Fe surfaces showing the RHEED streak splitting, the splitting disappears abruptly. One Cu(001) atomic layer is sufficient to remove any trace of it.

For Cu grown at room temperature on Fe(001) the RHEED streaks are sharp and the specular spot shows strong RHEED oscillations, see Fig. 2. The growth of bcc Cu on Fe(001) is epitaxial as is the Fe growth on Ag(001) but without the problems of vertical mismatch. The absence of RHEED streak splitting and the sharpness of the RHEED patterns indicate that the average atomic terrace width is significantly larger than that obtained for Fe grown on Ag(001) at RT. The width of RHEED streaks in the early stages of the Cu growth approaches that of the Ag(001) substrate and therefore the average separation between Cu(001) atomic terraces exceeds significantly 6 nm.

At a critical thickness of 11–12 ML, the Cu(001) over-

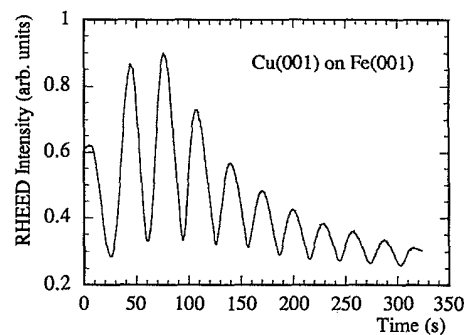


FIG. 2. RHEED intensity oscillations measured at the specular spot during the growth at room temperature of metastable bcc Cu(001) on bcc Fe(001). The electron beam angle of incidence was  $1^\circ$ , close to the first anti-Bragg condition.

layers start to undergo a weak but noticeable surface reconstruction.<sup>12</sup> A similar situation was observed in bcc Ni(001) overlayers where the critical thickness is much smaller (3–4 ML) and where the surface reconstruction is eventually accompanied by an appreciable lattice transformation.<sup>6,13</sup> Reconstructed Cu overlayers which are thicker than 12 ML most likely undergo a significant lattice transformation as well. The amplitude of RHEED intensity oscillations during the growth of Cu, see Fig. 2, gradually decreases with increasing thickness. This trend is even more pronounced as the critical thickness is approached. Therefore, it appears that the average atomic terrace width decreases with an increasing Cu thickness.

The surface of the first Fe layer grown at room temperature does not change sufficiently upon annealing (for 10–15 min) to produce any observable changes in the RHEED patterns. The RHEED streak splitting remains unchanged even at 510 K. The Ag Auger peak intensity measurements indicate that no appreciable interdiffusion between the Ag(001) substrate and a 6 ML-thick Fe layer occurs up to 470 K. However, the RHEED patterns change significantly when the growth is carried out at raised temperatures. In our sample preparation procedure the first 5–6 ML of Fe were grown at RT to protect the Ag/Fe interface from atomic intermixing. Then the substrate temperature was raised and 3–4 additional atomic layers of Fe were added. The growth at raised substrate temperatures exhibited a behavior which was similar to that observed during the growth of Fe on Fe whisker substrates.<sup>14</sup> The RHEED streak splitting of Fe on Ag(001) became more pronounced (sharper lines) and the separation between split lines decreased with increasing substrate temperature and disappeared completely for temperatures greater than 410 K, see Fig. 1(b). The amplitude of the RHEED intensity oscillations increased substantially,  $\sim 2$ – $3$  fold, see Fig. 3, compared with that observed during the growth at RT. The first period was definitely longer than subsequent periods which were regular and corresponded to 1 ML formation. At a substrate temperature of  $\sim 420$  K, Henzler's streak splitting of Fe disappeared after one additional atomic layer was deposited. The corresponding RHEED patterns were sharp and comparable with the best patterns observed.

In Fe/Cu/Fe trilayers with thin Cu interlayers (1–4

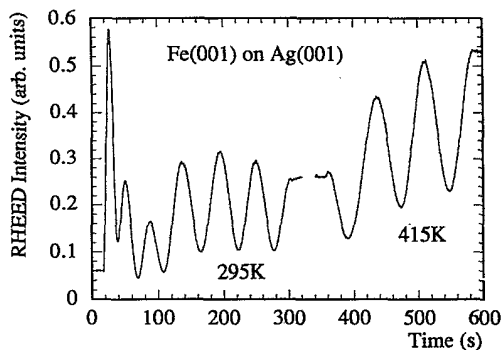


FIG. 3. RHEED intensity oscillations measured at the specular spot during the growth of bcc Fe(001) on a Ag(001) single-crystal substrate at 295 K and Fe(001) on an Fe(001) template at 415 K. The electron beam angle of incidence was  $1^\circ$ , close to the first anti-Bragg condition.

ML) deposited on Fe layers, which were prepared using raised substrate temperatures, the Fe/Cu and Cu/Fe interfaces consisted of large and comparable atomic terraces. With increasing Cu thickness the average terrace width in the Cu/Fe interface decreases and for thicknesses approaching the critical thickness (12 ML) it definitely becomes smaller than that at the Fe/Cu interface. Here we are using a notation in which Fe/Cu refers to a copper layer which was grown on an Fe(001) film and Cu/Fe refers to an iron layer which was grown on a Cu(001) film.

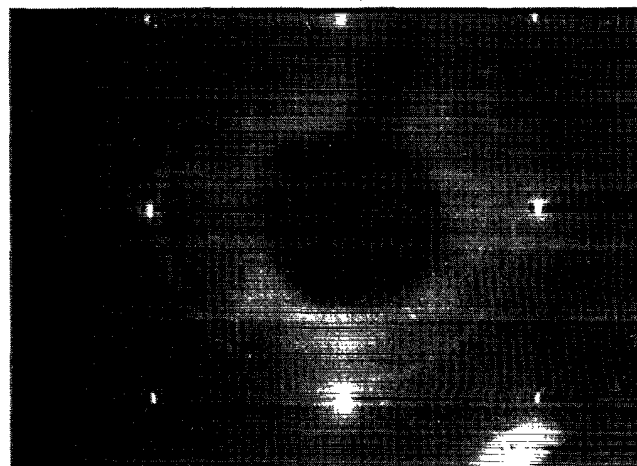
#### LEED STUDIES OF bcc Cu(001)

RHEED studies do not easily yield information on the vertical spacing between atomic layers and therefore we could not determine the vertical distortion of the Cu interlayers from the bcc stacking. For that reason additional LEED studies of Cu(001) on Fe(001) were carried out. Two epitaxial bcc Cu(001) films were grown on Fe(001) single-crystal whiskers for LEED studies. These layers were deposited in another multichamber MBE machine (VG Semicon V80M). The Fe whiskers were subjected to several cycles of Ar-ion sputtering at 1020 K and were then given a final anneal of 30–40 min at 970 K. Auger spectroscopy showed the presence of C (<2%) and O (<1%). Cu was evaporated at  $6 \text{ \AA}/\text{min}$  from a Knudsen cell. These depositions were monitored by means of RHEED oscillations. Two Cu layers were grown, 6 and 8.5 ML thick.

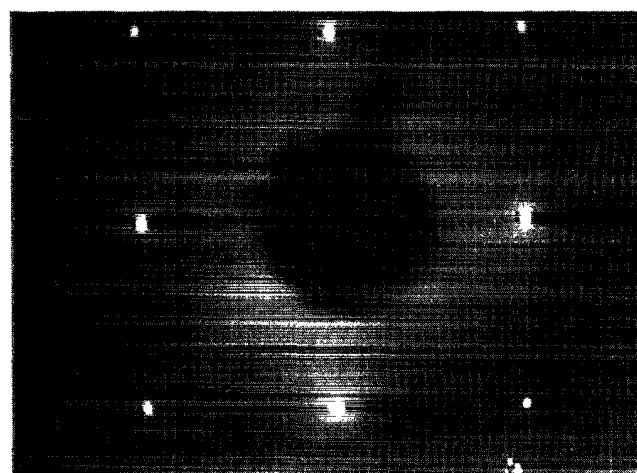
The Cu(001) layers showed well-defined LEED patterns at each stage, see Fig. 4. The symmetry and in-plane lattice spacing determined from the LEED patterns for Fe and Cu were precisely the same. The vertical spacing between the Cu(001) atomic layers was determined from the LEED  $e$ -beam energies for which there are enhancements along the (00) beams. At higher energies these corresponded quite well to simple Bragg reflections and can be used to determine the perpendicular lattice spacing from kinematic LEED theory.<sup>15</sup> The enhanced reflections appeared at energies  $E_n$ ,

$$E_n = 37.6 \left[ \frac{n}{a_\perp} \right]^2 + U_0 (\text{eV}), \quad (3)$$

where  $n$  is an integer,  $a_\perp$  is the distance between atomic planes perpendicular to the surface in  $\text{\AA}$ , and  $U_0$  is the average potential energy which is negative. Plots of energies at the main maxima of LEED intensity vs  $n^2$  are shown in Fig. 5 for an Fe(001) substrate and in Fig. 6 for 6- and 8.5 ML-thick Cu(001) layers. By fitting straight lines to these data we obtained  $a_\perp = 1.44 \text{ \AA}$  for both the Fe substrate and the Cu overlayers. The fits gave  $U_0 = -12 \text{ V}$  for the Fe and  $U_0 = -6$  to  $-11 \text{ V}$  for the 6 and 8.5 Cu layers, respectively. In both Fe and Cu additional weak maxima occurred between the main maxima for which no mechanism is presented here. They can be included in the data analysis if the indices are replaced by  $2n$ . The above LEED studies confirm that Cu(001) overlayers grown on Fe(001) templates are bcc with a lattice spacing equal to that of the bulk Fe.<sup>16</sup>



(a)



(b)

FIG. 4. LEED patterns: (a) Fe whisker; (b) 8.5 ML-thick Cu(001) layer grown on an Fe(001) whisker. LEED energy = 93 eV.

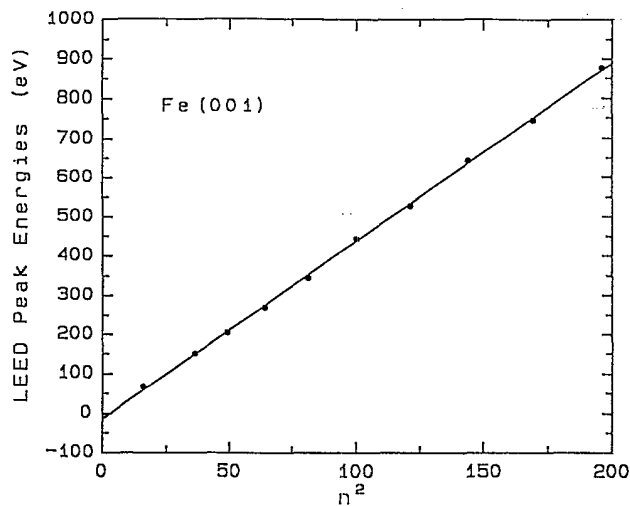


FIG. 5. The primary beam energies of the main LEED intensity maxima vs  $n^2$  [see Eq. (3)] for an Fe(001) whisker template.

### MAGNETIC STUDIES

Magnetic studies were carried out using ferromagnetic resonance and surface magneto-optical Kerr effect. The merits of both techniques and the interpretation of the measured data have been presented in detail in our recent paper.<sup>3</sup>

The studies in the present paper were restricted to samples in which two magnetic layers were separated by a Cu layer in which Cu maintained an unreconstructed bcc structure (2–12 ML thick) and therefore the measured exchange coupling was unobscured by the Cu layer lattice transformation. The Cu lattice transformation (see Growth Studies) very likely changes the Cu Fermi surface topology and consequently affects the exchange coupling.

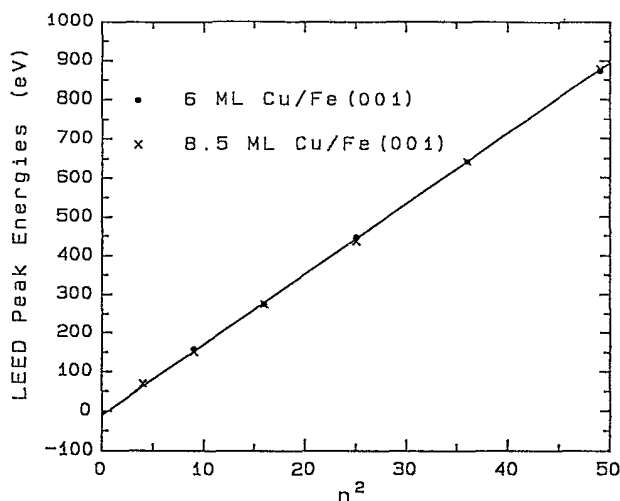


FIG. 6. The primary beam energies of the main LEED intensities vs  $n^2$  maxima [see Eq. (3)] for 6- and 8.5-ML-thick Cu(001) layers grown on an Fe(001) template.

### BILINEAR AND BIQUADRATIC EXCHANGE COUPLING

Typical SMOKE data for the applied field along one of the in-plane fourfold easy  $\{100\}$  axes are shown in Fig. 7. The polarization of the incident light is such that the magneto-optical signal (MO) signal is proportional to the magnetic moments along the direction of applied field (oriented along the easy axis in the plane of the film).

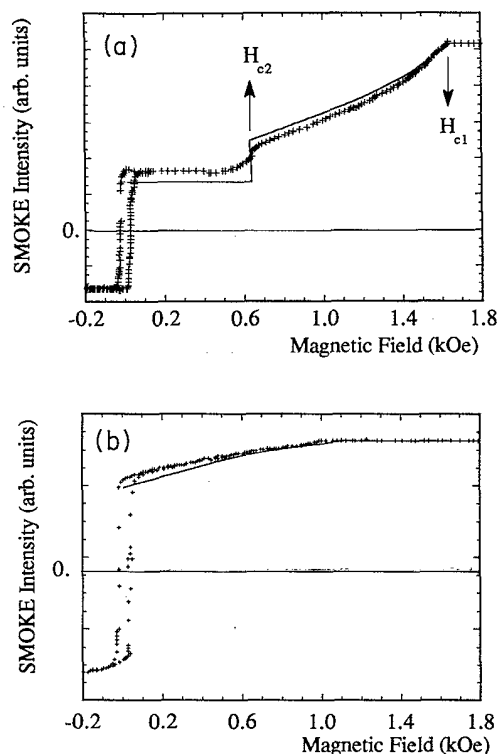


FIG. 7. Typical hysteresis loops measured by the SMOKE technique: (a) sample 9.4Fe/12Cu/16Fe. The applied field lies along the easy magnetic axis,  $\{100\}$  direction. Fields,  $H_{c1}$  and  $H_{c2}$  are clearly visible (see text) indicating that the exchange coupling is antiferromagnetic. The abrupt change near zero fields is due to magnetization reversal via domain walls. The solid line is a calculated curve using the following parameters:  $4\pi M_{\text{eff}}=6.08$  kG,  $2K_1/M_s=0.31$  kOe for the 9.4-ML Fe(001) layer;  $4\pi M_{\text{eff}}=15.52$  kG,  $2K_1/M_s=0.47$  kOe for the 16-ML Fe(001) layer;  $J_0=-0.237$  ergs/cm<sup>2</sup>,  $J_1=0.027$  ergs/cm<sup>2</sup> [see Eq. (2) in the text]. Observed and calculated intensities have been set equal at high magnetic fields. The discrepancy between the calculated and observed intensities at low magnetic fields is thought to be due mainly to the difference in optical properties between the iron and copper films. It is estimated that the structure behaves as if the iron film next to the substrate has been reduced in thickness by  $\sim 12\%$ . (b) Sample 9.4Fe/9Cu/16Fe. The applied field lies along the easy magnetic axis,  $\{100\}$  direction. The solid line is a calculated curve using the following parameters:  $4\pi M_{\text{eff}}=6.08$  kG,  $2K_1/M_s=0.31$  kOe for the 9.4 ML Fe(001) layer;  $4\pi M_{\text{eff}}=15.52$  kG,  $2K_1/M_s=0.47$  kOe for the 16-ML Fe(001) layer;  $J_0=-0.015$  ergs/cm<sup>2</sup>,  $J_1=0.1$  ergs/cm<sup>2</sup> [see Eq. (2) in the text]. Note that in this case the second critical field  $H_{c1}$  is not present and the magnetic moments are nearly perpendicular to each other in zero magnetic field.

Two critical fields are clearly visible in Fig. 7(a). The upper critical field,  $H_{c1}$ , corresponds to the field at which the magnetic moments of the individual Fe layers start to deviate from the direction of the dc external field. The second critical field,  $H_{c2}$ , corresponds to reaching an antiferromagnetic configuration along the easy axis in which the magnetization in the thicker layer lies in the field direction, and the magnetization in the thinner layer lies opposite to the field direction. If the magnetization loops are calculated using fourfold anisotropy and only bilinear exchange coupling, the main features of the observed loops are preserved, but two obvious differences become apparent. First, the calculated total magnetic moment along the applied field at the critical field  $H_{c1}$  shows a well-defined jump that is not observed in Fig. 7(a). Second, the observed position of the second critical field  $H_{c2}$  is usually at a lower field than that calculated from the value of the exchange coupling determined by  $H_{c1}$ . In fact, in some samples the second critical field is absent altogether and the total magnetic moment in zero applied magnetic field corresponds to a configuration in which the individual trilayer magnetic moments are nearly oriented along the mutually perpendicular easy magnetic axes ( $\{100\}$ ), see Fig. 7(b). This observation is not predicted if one uses only the bilinear term. Also one always needs to decrease the value of the antiferromagnetic exchange coupling with an increasing angle between the magnetic moments in order to bring  $H_{c2}$  into agreement with the measured value. This behavior was observed already in our first reported SMOKE measurements on Fe/Cu/Fe samples,<sup>12</sup> but it was not until later during the studies of fcc Co/Cu/Cu(001) (Ref. 3) that we explained the measured magnetization loops using an angular-dependent exchange coupling of the form

$$J = J_0 - J_1 \cos\Theta. \quad (4)$$

Positive  $J_1$  lowers the energy when the angle between the magnetizations is  $90^\circ$  [see Eq. (5) below]. Similar behavior was found also by Ruhring *et al.*<sup>2</sup> in Fe/Cr/Fe samples where they introduced the concept of a biquadratic exchange coupling

$$E = -J_0 \cos(\Theta) - J_1 \sin^2(\Theta). \quad (5)$$

Both descriptions are equivalent. Recently Slonczewski identified a possible origin for such behavior. He showed that interface roughness resulting in variations of the interlayer thickness together with short-wavelength oscillations (layer by layer) in the exchange coupling resulted in the presence of biquadratic exchange coupling. The strength of the biquadratic exchange coupling is given by<sup>1</sup>

$$J_1 = \frac{-2(\Delta J)^2 L}{\pi^3 A} g(f) \sum_{m=1}^{\infty} \left\{ \frac{\coth[\pi(2m-1)(D_1/L)]}{(2m-1)^3} + \frac{\coth[\pi(2m-1)(D_2/L)]}{(2m-1)^3} \right\}, \quad (6)$$

where  $A$  is the bulk exchange coupling constant,  $\Delta J$  is

one-half of the change in exchange coupling from odd to even ML (thus it is the slowly varying amplitude of the short-period oscillations),  $D_1$  and  $D_2$  are the thicknesses of the individual ferromagnetic layers,  $2L$  is the average distance between atomic terraces, see Fig. 8, and  $g(f)$  is a function of the partial coverage.

The field dependence of all of our magnetization loops measured by means of SMOKE are better described when biquadratic exchange is included. The biquadratic exchange term removes the jump in the calculated magnetic moment at  $H_{c1}$  and moves the second critical field  $H_{c2}$  towards lower dc fields. Even for the sample with 5.7-ML-thick Fe layers (possessing very small in-plane four-fold anisotropies), the field dependence of the magnetization loop deviates from linearity (for  $K_1 \ll J_0/d$ ) and the observed dependence can be explained by the presence of a small biquadratic exchange coupling. The results of our analyses are summarized in Table I. The values of bilinear and biquadratic exchange couplings obtained by fitting the magnetization loops are listed in the second and third columns. The fitting was carried out by assuming that the magnetization process follows the path of minimum energy.<sup>17</sup> For completeness, the fourth and fifth columns include the analyses in which the measured critical field  $H_{c1}$  is interpreted by assuming a bilinear exchange coupling only. The fourth column corresponds to the rotational magnetization process and the fifth column corresponds to a magnetization process following the path of minimum energy. The measured trilayers were mostly prepared with the Cu interlayer grown at RT. The substrate temperature during the Cu growth significantly affects the values of  $J_0$  and  $J_1$ , compare entries 1 with 2, 4 with 5, and 7 with 8 in Table I.  $J_1$  is increased by growing Cu above RT. The dependences of  $J_0$  and  $J_1$  on Cu layer thicknesses are shown in Fig. 9.

In samples grown at elevated temperatures the thickness dependence of the exchange coupling is similar to that observed in Fe/Cu/Fe trilayers which were entirely prepared at RT. However, there was a significant difference, see Fig. 10. The samples with the first Fe layer prepared at  $\sim 420$  K showed a distinct decrease in magnitude of the antiferromagnetic exchange coupling for an interlayer thickness of 10.5–11 ML ( $-0.16$  ergs/cm<sup>2</sup>). The exchange coupling is stronger at 10 ML ( $-0.2$  ergs/cm<sup>2</sup>) and at 12 ML ( $-0.22$  ergs/cm<sup>2</sup>). All

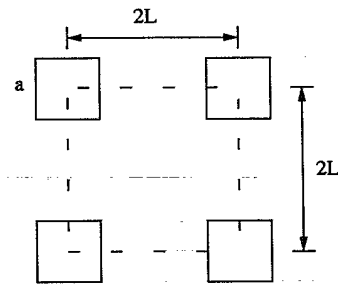


FIG. 8. Schematic diagram of the last layer fractionally covered. Clusters with an average area  $a^2$  are separated by an average distance  $2L$ .

Fe/Cu/Fe trilayers with a Cu interlayer thickness less than 9 ML showed only ferromagnetic coupling. Samples with a Cu interlayer thickness equal to or less than 7 ML showed only the acoustic FMR peak and therefore possessed strong ferromagnetic coupling.

#### COMPARISON OF FMR AND SMOKE MEASUREMENTS.

The strength of the antiferromagnetic exchange coupling was also studied by means of FMR. The evaluation of the exchange coupling from the FMR measurements is well described in our recent paper.<sup>3</sup> Values of the effective bilinear exchange coupling measured using FMR are listed in Table I, the sixth column.

FMR measurements were carried out in large dc magnetic fields (6–10 kOe) which significantly exceeded the critical field,  $H_{c1}$  (0.6–2 kOe), at which the magnetic moments start to deviate from saturation due to the antiferromagnetic coupling. In FMR the strength of the exchange coupling was measured and evaluated with the average static magnetic moments oriented parallel with the applied dc field. It is interesting to compare the values of the exchange coupling obtained from the FMR and SMOKE techniques. The fact that the FMR measurements were carried out in large dc fields makes this

comparison particularly interesting. The biquadratic exchange coupling is a consequence of small in-plane deviations of the dc magnetic moments from their average direction.<sup>1</sup> The applied dc field in FMR measurements decreases those deviations and could consequently result in a decreased value of the biquadratic exchange coupling. If the role of the applied field in FMR on the measured value of the biquadratic exchange coupling is negligible then the effective exchange coupling in FMR is  $J_0 - 2J_1$ . Note that the values of  $(J_0 - 2J_1)$  calculated from the second and third columns of Table I are very nearly equal to the effective bilinear exchange coupling obtained from the critical field  $H_{c1}$  and with the assumption that the magnetization follows the rotational process, see the fourth column in Table I. Except for the third and eighth entries listed in Table I, the values of the exchange coupling measured using FMR are less than  $J_0 - 2J_1$  and therefore it appears that the value of the biquadratic exchange coupling is decreased by the presence of the applied magnetic field. In fact, it is interesting to note that the effective exchange coupling measured by means of FMR is approximately equal to the effective bilinear exchange coupling obtained from the critical field  $H_{c1}$  and by assuming that the magnetization process follows the path of minimum energy, see the fifth column in Table I.

TABLE I. The results of the exchange coupling as a function of Cu interlayer thickness deduced from SMOKE and FMR measurements. All results listed are in units of ergs/cm<sup>2</sup>.  $J_0$  and  $J_1$  denote the bilinear and biquadratic exchange coupling, respectively, see Eqs. (2) and (4), and assuming the path of minimum energy using the following parameters:  $4\pi M_{\text{eff}} = 6.08$  kG,  $2K_1/M_s = 0.31$  kOe for a 9.4-ML Fe(001) layer; and  $4\pi M_{\text{eff}} = 15.52$  kG,  $2K_1/M_s = 0.47$  kOe for a 16-ML Fe(001) layer. Bilinear rotation and bilinear minimum denote exchange couplings which were calculated based on purely rotational processes or upon magnetization process which follow the path of minimum energy, respectively. FMR results denote the values of the exchange coupling determined from FMR measurements. Easy and hard indicates the easy ( $\{100\}$ ) and hard ( $\{110\}$ ) in-plane magnetic axes.

Sample and growth temperatures (K)	$J_0$	$J_1$	Bilinear rotation	Bilinear minimum	FMR results
(1) 9.4Fe/ 9Cu/ 16Fe 420 310 295	-0.059	0.055	-0.169	-0.152	-0.156
(2) 9.4Fe/ 9Cu/ 16Fe 420 340 295	-0.015	0.10	-0.215	-0.207	-0.192
(3) 9Fe/ 10Cu/ 16Fe 420 295 295	-0.084	0.060	-0.204	-0.195	-0.224
(4) 9.4Fe/10.5Cu/ 16Fe 400 295 295	-0.118	0.027	-0.172	-0.152	
(5) 9.4Fe/10.5Cu/ 16Fe 420 330 295	-0.070	0.050	-0.169	-0.155	
(6) 9.4Fe/ 11Cu/ 16Fe 420 330 295	-0.074	0.050	-0.174	-0.159	-0.163
(7) 9.4Fe/ 12Cu/ 17Fe 400 295 295	-0.198	0.017	-0.233	-0.220	-0.209
(8) 9.4Fe/ 12Cu/ 16Fe 430 325 295	Easy -0.237 Hard -0.221	0.027 0.035	-0.291 -0.283	-0.289 -0.281	-0.294
(9) 9.4Fe/ 14Cu/ 16Fe 420 295 295	-0.103	0.012	-0.137	-0.110	-0.110
(10) 5.7Fe/ 11Cu/ 5.7Fe 295 295 295	-0.193	0.010	-0.218	-0.218	-0.209
(11) 8.7Fe/10.5Cu/ 16Fe 295 295 295	-0.195	0.024	-0.243	-0.236	

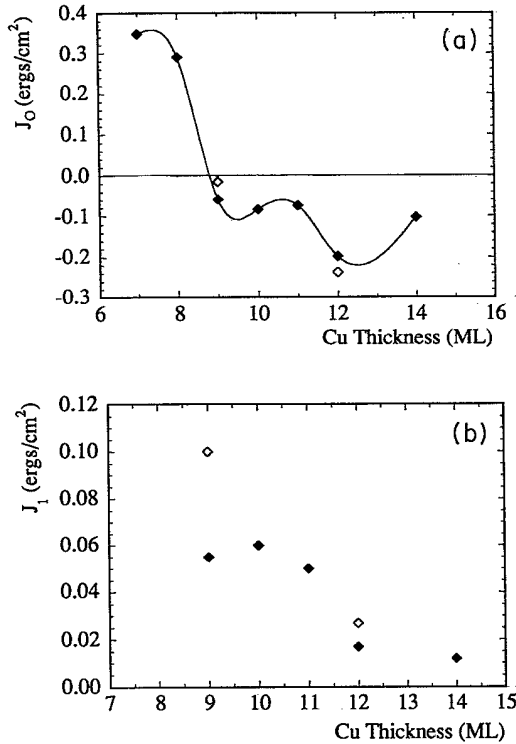


FIG. 9. (a) The bilinear exchange coupling,  $J_0$ , vs. Cu interlayer thickness (ML). (b) the biquadratic exchange coupling,  $J_1$ , vs Cu interlayer thickness. For 9 and 12 ML Cu two samples were prepared: the open symbols correspond to samples which were grown at raised Cu substrate temperatures (see Table I).

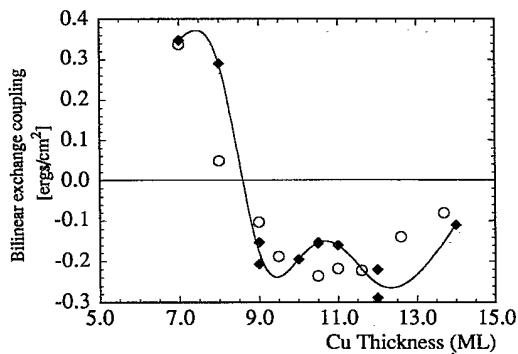


FIG. 10. The thickness dependence of the total bilinear exchange coupling  $J = J_0 - 2J_1$  in Fe/Cu/Fe trilayers measured at room temperature. Solid symbols correspond to trilayers with the first Fe layer grown at an elevated temperature ( $\sim 415$  K): open symbols correspond to samples grown entirely at room temperature. The open symbols represent the bilinear exchange coupling measured using the FMR technique (Ref. 5). The solid symbols in the AF region represent the bilinear exchange coupling determined from the critical field  $H_{c1}$  and assuming the path of minimum energy (see the fifth column of Table I): the solid symbols in the FM region were measured using FMR. The solid line (cubic spline fit) has been added to help guide the eye. The error in  $J$  and the interlayer thickness are smaller than the symbol size.

#### INTERPRETATION OF THE DATA USING THE SLONCZEWSKI MODEL

The rapid variation of the exchange coupling for the Cu interlayers 9–12 ML thick, see Figs. 9(a) and 10, and the presence of the biquadratic exchange coupling in all our measurements, see Fig. 9(b), strongly indicates that the exchange coupling in bcc Cu(001) has short-wavelength oscillations. It is therefore reasonable to explore the applicability of the Slonczewski model to our measurements. In the limit of small  $D/L$ , Eq. (6) can be rewritten in the form

$$J_1 = \Delta J \left\{ \frac{\Delta J}{M_s D} \right\} / \left\{ \frac{2Ak^2}{M_s} \right\}, \quad (7)$$

where  $k = \pi/L$ . This is a typical expression involving the phenomenon which is referred to as exchange narrowing (here more appropriately exchange averaging). Variations in the direction of the dc magnetic moment, caused by a fluctuating part of the exchange coupling field ( $\Delta J/M_s D$ ), are partly suppressed by the in-plane ferromagnetic exchange field ( $2Ak^2/M_s$ ). The  $k$  vector of the in-plane exchange field is given by the length scale of the lateral variations, which in the Slonczewski model is equal to  $2L$ . It follows that the fluctuating exchange coupling, ( $\Delta J$ ), is scaled down by the factor  $(\Delta J/M_s D)/(2A\pi^2/L^2 M_s)$ . In the limit of  $L \rightarrow 0$  the contribution to the biquadratic exchange disappears. This is a well-known feature of ultrathin structures: *A sample exhibiting fast spatial variations acquires properties corresponding to the average torque which in our case translates into the average bilinear exchange coupling.* More perfect interfaces exhibit a smaller ferromagnetic restoring torque and that results in a larger biquadratic exchange coupling. Our measured values of the biquadratic exchange coupling fully support this picture. The atomic terraces in the Cu/Fe interface become progressively smaller with an increasing Cu thickness, see the section Growth Studies. In the Slonczewski model smaller terraces correspond to a decreasing value of  $2L$ , and therefore  $2L$  is expected to decrease with increasing Cu thickness. This fact is directly reflected in the measured values of the biquadratic exchange coupling. The strength of the biquadratic exchange coupling  $J_1$  decreases with increasing Cu interlayer thickness, see Fig. 9(b).

Most of the Fe layer and Cu interlayer growths were terminated at the RHEED intensity maxima. We assume that their corresponding interfaces can be described by two atomic levels, see also the section Growth Studies. The Cu interlayer “ $N$  ML” thick has its interface formed by a completely filled  $N$ th layer but the  $N + 1$  layer is partially filled with mesas. Mesas occupy a fractional area  $f = a^2/(2L)^2$ , where  $a^2$  represents the average area of the mesas and  $2L$  represents the average distance between mesas, see Fig. 8. The growth studies showed that it is the second, Cu/Fe interface which has smaller terraces and therefore the above growth parameters describe the Cu/Fe interface. The Slonczewski model includes several parameters. The variations in the exchange cou-



pling are described by a parameter  $\Delta J = [J(N+1) - J(N)]/2$ , where  $J(N)$  represents the intrinsic exchange coupling through  $N$  atomic layers of Cu which would be measured in the absence of interface roughness. The interface roughness is described by two sets of parameters: (1) The parameters  $L(N)$  describe the length scale in which atomic terraces are distributed across the interface, see Fig. 8. (2) The parameters  $f(N)$  are fractional coverages for each thickness.

The idea is to identify the intrinsic bilinear exchange coupling  $J(N)$  from measured values of  $J_0(N)$  and  $J_1(N)$ . In order to do this we need additional information for  $f(N)$  or  $L(N)$ . We decided to start by choosing the fractional coverages  $f(N)=0.3$ . The initial choice of  $f(N)=0.3$  was found to lead to a divergent behavior of  $\Delta J$  with increasing Cu thickness. To avoid that we had to increase  $f(N)$  with layer number: We used the set  $f=0.3, 0.3, 0.3, 0.3, 0.35, 0.4$  for Cu interlayers 7, 8, 9, 10, 11, and 12 ML thick, respectively.

The measured bilinear exchange coupling is given by

$$J_0(N) = J(N) + \{J(N+1) - J(N)\}f, \quad (8)$$

and the biquadratic exchange coupling is given by formula (6). In order to determine  $J(N)$  and  $L(N)$  one has to identify one additional parameter. The bilinear exchange coupling strength is slowly varying for Cu interlayer thicknesses of 10–11 ML, see Fig. 9(a). Therefore, we used  $L$  for 10 ML-thick Cu as an additional parameter [ $L(10)$ ] which allowed us then to determine the values of  $J(N)$  and  $L(N)$  for all the other samples measured. Using Eqs. (6) and (8) one can determine values for  $J(10)$  and  $J(11)$ . This approach then allows one to propagate the analysis. Equation (8) determines  $J(N)$  and Eq. (6) allows us to evaluate  $L(N)$  for a given Cu interlayer. The results of such an analysis are summarized in Table II for three different preselected values of  $L(10)$  (100, 200, and 300 Å). The exchange coupling  $J(N)$  always shows an os-

cillatory behavior, see Fig. 11. A decreasing value of the biquadratic exchange coupling and an increasing value of  $\Delta J = [J(N+1) - J(N)]/2$  with increasing Cu thickness leads to a rapid decrease of  $L$  with increasing Cu interlayer thickness, see Table II. The choice of  $L(10)=100$  Å leads to very short terrace separation  $2L$  for samples with 11 and 12 ML Cu (35 and 10 Å). The RHEED patterns for these samples are not appreciably broadened, hence this particular case has to be considered unrealistic. Calculated values of  $L$  increase with an increasing value of  $L(10)$ . Because the choice of  $L(10)=300$  Å leads to a rather large value of  $L(730$  Å) for 9 ML-thick Cu, the choice of 200 Å for  $L(10)$  seems to be more appropriate.

In all analyses the values of  $L$  decreases rather rapidly with increasing Cu thickness, but the RHEED patterns do not provide any evidence for such a rapid change in surface roughness with increasing Cu thickness. It is therefore important to find out whether the Slonczewski model is able to predict a more realistic behavior. Calculations show that an increased partial coverage,  $f$ , results in a more gradual change of  $L$  with Cu thickness. An analysis was carried out using  $f=0.5$  for all Cu interlayers, and using  $L(10)=100, 150,$  and  $200$  Å. The results are shown in Table III. The parameter  $L$  decreases again with an increasing Cu thickness but this dependence is much slower than that in the first case. The thickness dependence of the bilinear exchange coupling  $J(N)$  exhibits short-wavelength oscillations, see Fig. 12. Note that the exchange coupling  $J(13)$  is less than  $J(12)$  as expected from the measured overall thickness dependence of the exchange coupling. This shows again that the choice  $f=0.5$  is very realistic. At this point one would like to find some additional evidence which supports such a choice. The partial coverage  $f=0.5$  implies that " $N$ " ML Cu corresponds to a total Cu coverage of  $(N+0.5)$  ML. This particular point is easy to verify.

TABLE II. The exchange interaction for "structurally perfect" Fe/Cu/Fe trilayers as a function of the Cu interlayer thickness. The analyses were carried out on a subset of samples (with the first Fe layer grown at raised substrate temperatures) listed in Table I. The results of the analysis were obtained from the measured values of the bilinear and biquadratic exchange coupling terms by an application of the Slonczewski model (Ref. 1). See details in the text. The pairs of  $J(N)$  and  $L(N)$  were evaluated by using  $L(10)=100, 200,$  and  $300$  Å, respectively. The underlined entries correspond to samples in which the Cu interlayer was grown at a higher substrate temperature: In these underlined samples the bilinear exchange coupling was evaluated by using the values  $J(N)$  for  $L(10)=200$  Å and adjusting appropriately the coverage  $f$ ;  $f=0.19$  and  $0.38$  for Cu interlayers 9 and 12 ML thick, respectively.

Cu thickness (ML)	$f$	$J(N)$ $\left[ \frac{\text{ergs}}{\text{cm}^2} \right]$	$L$ (Å)	$J(N)$ $\left[ \frac{\text{ergs}}{\text{cm}^2} \right]$	$L$ (Å)	$J(N)$ $\left[ \frac{\text{ergs}}{\text{cm}^2} \right]$	$L$ (Å)
7.0	0.30	0.38		0.331		0.325	
8.0	0.30	0.279		0.394		0.41	
9.0	0.30	0.326	180	0.076	410	0.021	540
<u>9.0</u>		0.326	240	0.076	550	0.02	730
10.0	0.30	-0.564	100	-0.33	200	-0.246	300
11.0	0.35	1.03	35	0.49	85	0.294	140
12.0	0.40	-2.040	6	-1.1	25	-0.746	50
<u>12.0</u>		-2.04	10	-1.1	35	-0.746	70
13.0		2.56		1.16		0.624	

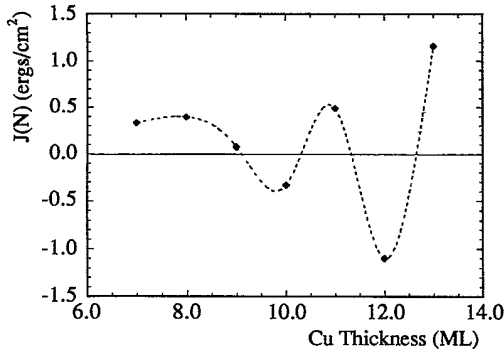


FIG. 11. Values deduced for the thickness dependence of the exchange coupling  $J(N)$  which pertain to a smooth interface. These coupling strengths have been calculated from the data using the Slonczewski model (Ref. 1) assuming  $f=0.3, 0.3, 0.3, 0.3, 0.35, 0.4$  for 7, 8, 9, 10, 11, and 12 ML Cu respectively, and  $L(10)=200 \text{ \AA}$  (see the text). The solid line is a cubic spline fit to guide the eyes.

The RHEED intensity oscillations allow one to determine the overlayer thickness. We have found in all our growth studies that the period of the RHEED oscillations corresponding to 1 ML formation (stationary period) is observed only after several initial oscillations. The first few oscillations involve a phase slip which results in a longer period. Therefore, the total thickness of a given film in ML can be determined by dividing the total growth time (for constant evaporation rate) by the stationary period. Using this approach one finds, see Fig. 2, that the Cu interlayer terminated at the  $N$ th RHEED maximum indeed corresponds to the thickness  $N+0.5$  (in ML) as was used in the analysis of the exchange coupling. A sample which displays  $N$  RHEED oscillations represents a coverage of  $N+0.5$  ML. The RHEED oscillations cannot be used to determine the distribution of atoms in the top layers. The presence of oscillations indi-

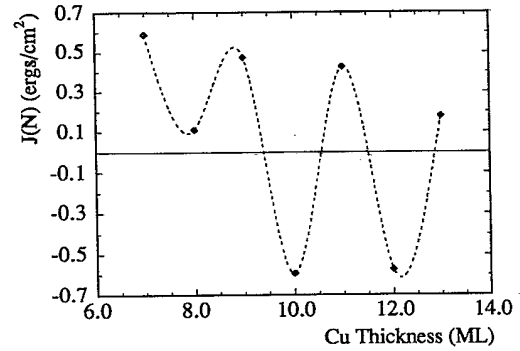


FIG. 12. Values deduced for the thickness dependence of the exchange coupling  $J(N)$  which pertain to a smooth interface. These couplings strengths have been calculated from the data using the Slonczewski model (Ref. 1) assuming  $f=0.5$  for all Cu interlayers, and  $L(10)=150 \text{ \AA}$  (see the text). The solid line is a cubic spline fit to guide the eyes.

cates strongly that only the last two top atomic layers are partially filled but RHEED oscillations do not allow one to determine the coverages of the last two atomic layers. Growth modeling leads to the conclusion that there will be some pits in the " $N$ th" ML. This was ignored in applying the Slonczewski model because it deals with only two layers. But it matters not whether there are pits or mesas; in one case we would use  $2\Delta J = |J(N) - J(N-1)|$  and in the other  $2\Delta J = |J(N+1) - J(N)|$ . For the case  $f=0.5$  these two values are nearly the same. The Slonczewski model then would say that  $f$  is the sum of the pits and the mesas. It would be interesting to check the actual distribution of pits and mesas using STM.

The exchange coupling,  $J(N)$ , corresponding to a perfect interface shows strong short-wavelength ( $\sim 2, 2$  ML) oscillations independent of the particular choice of  $f(N)$ . Herman, Sticht, and van Schilfgaarde<sup>4</sup> have carried out

TABLE III. The exchange interaction for "structurally perfect" Fe/Cu/Fe trilayers as a function of the Cu interlayer thickness. The analyses were carried out on a subset of samples (with the first Fe layer grown at raised substrate temperatures) listed in Table I. The results of the analysis were obtained from the measured values of the bilinear and biquadratic exchange coupling terms by an application of the Slonczewski model (Ref. 1). See details in the text. The pairs of  $J(N)$  and  $L(N)$  were evaluated by using  $L(10)=100, 150,$  and  $200 \text{ \AA}$ , respectively. The underlined entries correspond to samples in which the Cu interlayer was grown at a higher substrate temperature: In these underlined samples the bilinear exchange coupling was evaluated by using the values  $J(N)$  for  $L(10)=150 \text{ \AA}$  and adjusting appropriately the coverage  $f$ ;  $f=0.46$  and  $0.45$  for Cu interlayers 9 and 12 ML thick, respectively.

Cu thickness (ML)	$f$	$J(N)$ $\left[ \frac{\text{ergs}}{\text{cm}^2} \right]$	$L$ ( $\text{\AA}$ )	$J(N)$ $\left[ \frac{\text{ergs}}{\text{cm}^2} \right]$	$L$ ( $\text{\AA}$ )	$J(N)$ $\left[ \frac{\text{ergs}}{\text{cm}^2} \right]$	$L$ ( $\text{\AA}$ )
7.0	0.50	0.818		0.59		0.464	
8.0	0.50	-0.118		0.11		0.237	
9.0	0.50	0.704	91	0.476	134	0.349	178
<u>9.0</u>		0.704	127	0.564	183	0.45	240
10.0	0.50	-0.82	100	-0.594	150	-0.467	200
11.0	0.5	0.654	91	0.426	137	0.30	185
12.0	0.50	-0.802	60	-0.574	104	-0.448	160
<u>12.0</u>		-0.802	80	-0.574	117	-0.448	190
13.0	0.50	0.406		0.178		0.052	

first-principles calculations of the exchange coupling through bcc Cu in Fe/Cu/Fe structures. The thickness dependence of the exchange coupling, see Fig. 1 in Ref. 4 shows a behavior similar to that observed in our measurements, Figs. 9(a) and 10. This similarity is even more obvious if their calculations are compared with Figs. 11 and 12. The first-principles calculations by Herman, Sticht, and van Schilfgaarde show that the exchange coupling crosses from ferromagnetic to antiferromagnetic coupling at  $d_{\text{Cu}}=8 \text{ \AA}$ , and then a rapid variation in the antiferromagnetic coupling occurs with a separation between antiferromagnetic maxima of  $3.4 \text{ \AA}$  (2.4 ML). The antiferromagnetic coupling strength reaches maximum values near 8 and  $12 \text{ \AA}$  with a slightly positive ferromagnetic coupling in between (at  $10 \text{ \AA}$ ). Our values for  $J(N)$  show a similar trend. The measured periodicity (2.2 ML) of short-wavelength oscillations is very close to those obtained from the first-principle calculations by Herman, Sticht, and van Schilfgaarde (2.4 ML). The significant difference between the measured results and the calculations appears to be in the first crossover from ferromagnetic to antiferromagnetic coupling. The measurements show that this first crossover occurs for 9–10 ML-thick Cu. The first-principles calculations show the crossover at approximately 5.5 ML of Cu. We do not intend at this point to discuss this difference.

The strength of the oscillatory exchange coupling  $J(N)$ , see Figs. 11 and 12, is similar to that calculated by Bruno and Chappert<sup>18</sup> for fcc Cu(001) ( $0.4 \text{ ergs/cm}^2$ ). The first principles calculations for bcc Fe/Cu/Fe(001) by Herman, Shicht, and van Schilfgaarde gave significantly larger values for the exchange coupling ( $25 \text{ ergs/cm}^2$ ). Deaven, Rokhsar, and Johnson,<sup>19</sup> showed that it is difficult to obtain correct quantitative results for the amplitude of the oscillations but that the period of the oscillations is usually well described by present theoretical methods.

Slonczewski's model assumes that the exchange interaction provides the only field which keeps the saturation magnetization in each individual layer closely aligned along the common magnetization axis. It is prudent to ask at this point if this assumption is satisfied in our analysis. The parameter  $L$  for  $f=0.5$  is approximately  $200 \text{ \AA}$ , which gives the exchange field  $2Ak^2/M_s \sim 6 \text{ kOe}$ . This field is appreciably larger than any other field involved in SMOKE measurements and therefore the use of Eqs. (6) and (7) is fully justified. In FMR measurements, the applied magnetic field is comparable to the exchange field and therefore one could expect some decrease in the biquadratic exchange coupling in the FMR studies, see the section Comparison of FMR and SMOKE Studies.

Several points can be addressed at this time. It is interesting to note that the value of the bilinear exchange coupling for 10.5 ML-thick Cu was found to be nearly the same as that of the 10- and 11 ML-thick Cu layers. The fractional coverage in this sample cannot be represented by a surface with only one partially filled atomic layer. A thickness of 10.5 ML corresponds to a growth which has been terminated at a RHEED oscillation intensity minimum. A RHEED intensity minimum

corresponds to maximum surface roughness, and in this case there are two incomplete layers covering a filled layer, see Fig. 13. Three atomic layers are involved in the bilinear exchange coupling. The measured bilinear exchange coupling can be written in terms of the  $J(N)$ ,

$$\begin{aligned} J_0(N + \frac{1}{2}) = & J(N)(1 - f_1) + J(N + 1)(f_1 - f_2) \\ & + J(N + 2)f_2, \\ f_1 + f_2 = & 1 \text{ for } f = 0.5, \end{aligned} \quad (9)$$

where  $f_1$  and  $f_2$  are partial fillings of the top two atomic Cu layers. Using this formula with previously determined values of the exchange coupling for perfect surfaces  $J(10)$ ,  $J(11)$ , and  $J(12)$  [ $-0.594$ ,  $0.426$ ,  $-0.574 \text{ ergs/cm}^2$  for  $f=0.5$  and  $L(10)=150 \text{ \AA}$ ], one calculates for the two 10.5 ML-thick Cu samples (see entries 4 and 5 in Table I)  $f_1=0.73$ ,  $0.76$  and  $f_2=0.27$ ,  $0.24$ . The resulting coverages  $f_1$  and  $f_2$  are very reasonable. The eleventh ML increases its coverage by 0.25 and the twelfth ML gets partly filled,  $f_2=0.25$ . Note that the twelfth ML requires half of the coverage which would be obtained if the growth were to be terminated at the eleventh RHEED maximum.

Since the width of RHEED streaks for the Fe and Cu overlayers grown on iron deposited at an elevated temperature is mainly determined by the Ag(001) substrate mosaic spread, it is hard to determine the terrace width from RHEED streak patterns only. However, the samples which were grown entirely at RT showed a well-defined splitting of the RHEED streaks which allows one to estimate the average separation between the atomic mesas,  $2L$ , see the section Growth Studies. Therefore, it is interesting to find out whether the measured values of the biquadratic exchange coupling in those samples are in agreement with the above analysis. The sample 5.7Fe/11Cu/5.7Fe, see Table I, was entirely grown at room temperature. Its biquadratic exchange coupling was found to be  $J_1=0.01 \text{ ergs/cm}^2$ . Using the values for  $J(11)$  and  $J(12)$  ( $-0.594$  and  $0.426 \text{ ergs/cm}^2$ ), which were determined above, see Fig. 12, one can estimate from the measured value  $J_1$  the parameter  $2L$ . Equation (6) leads to  $85 \text{ \AA}$ . This estimate is very close to the average terrace separation which was determined from the RHEED streak splitting. One can also use formula (8) to interpret the corresponding value of  $J_0$  observed in this sample. The partial coverage required is  $f=0.6$ . The 0.6 coverage is then the sum of holes and pits.

Recent calculations by Edwards<sup>20</sup> showed that the biquadratic exchange coupling can be also generated by an intrinsic mechanism. In model calculations it is predict-

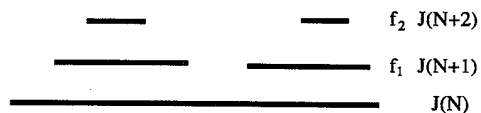


FIG. 13. Schematic diagram of partly filled atomic layers for a growth which was terminated at a RHEED intensity minimum, see the text.

ed that it can be equal to approximately  $\frac{1}{8}$  (12%) of the bilinear contribution. In our samples the biquadratic exchange coupling is very thickness dependent and can be comparable to the bilinear counterpart. Slonczewski's mechanism is definitely a major contributor to the strength of the biquadratic exchange coupling. However, for those samples which exhibit a small biquadratic exchange coupling part of this coupling term could be intrinsic in origin. The analysis of the data would not be changed in an appreciable way. The Slonczewski's contribution would be decreased by the contribution arising from the intrinsic contribution and this would require a decrease of the terrace separation  $2L$ . One can try to estimate the value of the intrinsic biquadratic exchange by choosing a reasonable value for the terrace separation. An acceptable choice of  $2L = 100 \text{ \AA}$  for a sample with a 12 ML Cu thick interlayer would require a decrease of the Slonczewski contribution by a factor 2 and therefore approximately half of the measured biquadratic exchange coupling for the 12 ML Cu sample could be ascribed to the intrinsic contribution ( $0.008 \text{ ergs/cm}^2$ ). This would suggest an intrinsic biquadratic exchange coupling which is approximately 5% of the bilinear contribution.

#### EXCHANGE COUPLING THROUGH Cu/Ag(001) INTERLAYERS

The exchange coupling between iron layers separated by Ag(001) or Au(001) exhibited very unusual behavior despite the fact that their Fermi surfaces are very similar to that of Cu.<sup>5</sup> In samples of Fe/Ag/Fe(001) grown at RT, the exchange coupling rapidly disappeared with Ag thickness. For Ag(001) interlayers thicker than 7 ML the exchange coupling was too weak to be observable. This unusual behavior was further investigated by inserting Ag(001) atomic layers epitaxially into Cu(001) interlayers. Several samples were grown with one and two Ag(001) atomic layers inserted at various locations in the Cu(001) interlayer, see Table IV. In all cases the presence of one Ag atomic interlayer resulted in a substantial decrease of the antiferromagnetic exchange coupling. Two Ag(001) atomic layers even led to a small ferromagnetic coupling. It is interesting to note that two Ag(001) atomic layers block a direct path between the Cu and the Fe atoms. Note that Ag does not alloy with Cu and therefore the hybridization between Cu and Ag is weak. This fact could imply that the Ag(001) atomic layers create a mismatch in the interlayer valence electron wave functions which results in a significant change of the exchange coupling. In all cases the presence of Ag resulted in a broadening of the FMR linewidths associated with both Fe layers (from 80 to 240 Oe in the 16 ML Fe and from 170 to 320 Oe in the 9.5 ML Fe): this indicates that the role of Ag is more complicated than would be expected from a mere decrease of the exchange coupling. One could argue that the broadening of the FMR linewidth is caused by a fluctuating exchange coupling across the sample. The observed broadening would correspond to a fluctuating exchange coupling of  $\sim 0.01 \text{ ergs/cm}^2$ . It is interesting to point out that both peaks are broadened almost equally (from their FMR linewidths which were

TABLE IV. The exchange coupling in Fe/Cu/Ag/Fe structures at 295 and 77 K. All results listed are in units of  $\text{ergs/cm}^2$ .  $J$  is the bilinear exchange coupling deduced from FMR. The numbers listed below the sample compositions indicate the growth temperature for each layer. Positive  $J$  indicates ferromagnetic coupling.

Sample and growth temperature (K)	$J$ at 295 K	$J$ at 77 K
9.4Fe/14Cu/1Ag/16Fe 420 340 300 300	-0.084	
9.4Fe/9Cu/2Ag/16Fe 420 340 310 295	0.07	0.1
9.4Fe/5Cu/2Ag/5Cu/14Fe 420 295 295 295 295	0.125	0.3
9.4Fe/10Cu/2Ag/15Fe 420 340 300 300	0.05	0.06

measured in the individual layers) which suggests that the exchange coupling is present and is indeed weak. This conclusion is further supported by the FMR intensities which are proportional to the total magnetic moment in the layer. The presence of the exchange coupling between layers changes the intensity ratio between the optical and the acoustic peak in FMR measurements.<sup>6</sup> From entries 2 and 4 in Table IV the intensity ratio of the two FMR peaks was found to be  $\sim 1.2$  which corresponds to a weak ferromagnetic coupling.

The decrease of the exchange coupling by a few ML of Ag in Fe/Cu/Ag/Fe films is most likely caused by the valence band mismatch between Cu and Ag. However, one should point out that the presence of a Ag layer can also lead to a very effective averaging out of the exchange coupling due to interface roughness. The importance of the interface averaging is supported by our studies of the exchange coupling in more recently prepared Fe/Ag/Fe samples<sup>21</sup> which have improved interfaces and which exhibit a very symmetric oscillatory exchange coupling.<sup>22</sup> Similar results were obtained recently by the NIST group using SEMPA measurements.<sup>23</sup> The Fe/Ag/Fe samples entirely grown at RT are accompanied by mismatched interface terraces. The first Fe/Ag interface has significantly shorter terraces than the second Ag/Fe interface (see Growth Studies). In these films the exchange coupling was equal to zero for Ag interlayers thicker than 7 ML. This behavior is most likely caused by an averaging effect of the exchange interaction. Further studies will be needed to disentangle the Cu, Ag valence band mismatch contribution from the effect of exchange coupling averaging which is caused by rough interfaces.

#### CONCLUSIONS

It has been shown that the average atomic terrace width in Fe/Cu/Fe trilayers can be significantly increased by increasing the substrate temperature during the growth of the first Fe layer. LEED data were presented in which it was shown that unreconstructed bcc Cu(001) grows in a bcc structure which imitates that of the bcc Fe(001) substrate.

The exchange coupling in Fe/Cu/Fe trilayers was studied as a function of the Cu interlayer thickness. The studies were carried out using the FMR and SMOKE techniques. Quantitative data from both techniques were in good agreement. The magnetization loops for Fe/Cu/Fe trilayers can only be well explained by including biquadratic exchange coupling. Values for the bilinear and biquadratic exchange coupling terms were determined from a detailed analysis of the observed magnetization loops. It has been shown that contrary to intuitive expectations the strength of the biquadratic exchange coupling term increases with increasing terrace width.

A quantitative analysis of the measured bilinear and biquadratic exchange coupling contributions was carried out using the Slonczewski model<sup>1</sup> for biquadratic exchange coupling. It has been shown that the exchange coupling  $J(N)$  for  $N$  perfectly smooth monolayers exhibits an oscillatory behavior. Its amplitude has been estimated. The observed thickness dependence of the exchange coupling has been compared with the recent first-principles calculations by Herman, Sticht, and van Schilf-gaarde.<sup>4</sup> The measured period (2.2 ML) of short-

wavelength oscillations is very close to that (2.4 ML) calculated in the first-principles calculations by Herman, Sticht, and van Schilf-gaarde.<sup>4</sup> Recent studies by Johnson *et al.*<sup>24</sup> of the exchange coupling on Fe whisker/Cu/Fe(001) samples showed also a maximum of the antiferromagnetic coupling for even numbers of Cu(001) ML.

The results of the measurement of the exchange coupling through composite Cu/Ag(001) interlayers have been presented. It is shown that the presence of a few atomic layers of Ag(001) very rapidly removes the antiferromagnetic exchange coupling. This rapid decrease is most likely caused by the mismatch between the valence electron states of Cu and Ag, but a spatial averaging over imperfect Ag(001) interfaces can also play a partial role.

#### ACKNOWLEDGMENT

The authors would like to thank the Natural Sciences and Engineering Research Council of Canada for grants that supported this work.

\*Present address: Physics Department, University of Lyon, France.

<sup>1</sup>J. C. Slonczewski, Phys. Rev. Lett. **67**, 3172 (1991).

<sup>2</sup>M. Rühlig, R. Schäfer, A. Hubert, R. Mosler, J. A. Wolf, S. Demokritov, and P. Grünberg, Phys. Status Solidi A **125**, 635 (1991).

<sup>3</sup>B. Heinrich, J. Kirschner, M. Kowalewski, J. F. Cochran, Z. Celinski, and A. S. Arrott, Phys. Rev. B **44**, 9348 (1991).

<sup>4</sup>F. Herman, J. Sticht, and M. van Schilf-gaarde, Mat. Res. Soc. Symp. Proc. **231**, 195 (1992).

<sup>5</sup>Z. Celinski and B. Heinrich, J. Magn. Magn. Mater. **99**, L25 (1991).

<sup>6</sup>B. Heinrich, S. T. Purcell, J. R. Dutcher, J. F. Cochran, and A. S. Arrott, Phys. Rev. B **38**, 12 879 (1988).

<sup>7</sup>B. Heinrich, A. S. Arrott, J. F. Cochran, Z. Celinski, and K. Myrtle, *Science and Technology of Nanostructured Magnetic Materials*, NATO Advanced Study Institute, edited by G. Hajipanais and G. A. Prinz and (Plenum, New York, 1991), p. 15.

<sup>8</sup>P. Hahn, J. Clabes, and M. Henzler, J. Appl. Phys. **51**, 2079 (1980).

<sup>9</sup>R. L. Lyles, Jr., S. J. Rothman, and W. Jager, Metallography **11**, 363 (1978).

<sup>10</sup>J. Kirschner (private communication).

<sup>11</sup>H. Li, Y. S. Li, J. Quinn, D. Tian, J. Sokolov, F. Jona, and P. M. Marcus, Phys. Rev. B **42**, 9195 (1990).

<sup>12</sup>B. Heinrich, Z. Celinski, J. F. Cochran, W. B. Muir, J. Rudd, Q. M. Zhong, A. S. Arrott, K. Myrtle, and J. Kirschner, Phys. Rev. Lett. **64**, 673 (1990).

<sup>13</sup>D. J. Jiang, N. Alberding, A. J. Seary, B. Heinrich, and E. D. Crozier, Physics B **158**, 662 (1989).

<sup>14</sup>A. S. Arrott, B. Heinrich, and S. T. Purcell, in *Kinetics of Ordering and Growth at Surface*, edited by M. G. Lagally (Plenum, New York, 1990), p. 321.

<sup>15</sup>J. B. Pendry, *Low Energy Electron Diffraction* (Academic, London, 1974), p. 23.

<sup>16</sup>However, the vertical distortion depends on structural details. Surface extended x-ray fine-structure (SEXAFS) studies on Cu(001) overlayers grown on Ag(001) substrates and covered by Au(001) showed that an appreciable vertical expansion (7.6%) is present in these structures. See D. T. Jiang, D. Crozier, and B. Heinrich, Phys. Rev. B **44** 6401 (1991).

<sup>17</sup>B. Dieny, J. P. Gavigan, and J. P. Rebouillat, J. Phys C **2**, 159 (1990); B. Dieny and J. P. Gavigan, *ibid.* **2**, 187 (1990).

<sup>18</sup>P. Bruno and C. Chappert, Phys. Rev. Lett. **67**, 1602 (1991).

<sup>19</sup>D. M. Deaven, D. S. Rokhsar, and M. Johnson, Phys. Rev. B **44**, 5977 (1991).

<sup>20</sup>D. M. Edwards, J. Mathon, R. B. Muniz, Murielle Villeret, and J. M. Ward, in *NATO Advanced Study Institute, Magnetism and Structure in Systems of Reduced Dimension*, edited by R. F. C. Farrow (Plenum, New York, to be published).

<sup>21</sup>The first 5 ML of Fe(001) were grown at room temperature, and the subsequent 3 ML were grown at 150°C. The remaining structure was grown at room temperature.

<sup>22</sup>Z. Celinski, B. Heinrich, and J. F. Cochran, J. Appl. Phys. (to be published).

<sup>23</sup>D. T. Pierce, J. Unguris, and R. J. Cellota, in *Ultrathin Magnetic Structures*, edited by B. Heinrich and J. A. C. Bland (Springer-Verlag, Berlin, to be published).

<sup>24</sup>M. T. Johnson, S. T. Purcell, N. W. E. McGee, R. Coehoorn, J. aan de Stegge, and W. Hoving, Phys. Rev. Lett. **68**, 2688 (1992).